

**Crystal-electric-field effects and quadrupole fluctuations in  $\text{Ce}_3\text{Au}_3\text{Sb}_4$  detected by Sb NQR**S.-H. Baek,<sup>1,\*</sup> H. Sakai,<sup>1,2</sup> H. Lee,<sup>1</sup> Z. Fisk,<sup>1,3</sup> E. D. Bauer,<sup>1</sup> and J. D. Thompson<sup>1</sup><sup>1</sup>*Los Alamos National Laboratory, Los Alamos, New Mexico 87545, USA*<sup>2</sup>*Advanced Science Research Center, Japan Atomic Energy Agency, Tokai, Ibaraki 319-1195, Japan*<sup>3</sup>*Department of Physics & Astronomy, University of California, Irvine, California 92697, USA*

(Received 14 December 2009; revised manuscript received 16 June 2010; published 7 July 2010)

We report <sup>121,123</sup>Sb nuclear quadrupole resonance (NQR) studies on single crystals of the narrow-gap semiconductor  $\text{Ce}_3\text{Au}_3\text{Sb}_4$ . Five NQR lines from the two Sb isotopes were successfully identified. The temperature dependence of the nuclear quadrupole frequency ( $\nu_Q$ ), as well as the static magnetic susceptibility ( $\chi$ ), is well explained by crystal-electric-field effects. The nuclear spin-lattice relaxation rates ( $T_1^{-1}$ ) of both <sup>121</sup>Sb and <sup>123</sup>Sb increase rapidly with decreasing temperature. The ratio of  $T_1^{-1}$  for the two Sb isotopes is constant at high temperature but it decreases at low temperatures, indicating the role of quadrupole fluctuations of the Ce ions. The possible origin of the large specific heat at low temperatures is discussed basing on our results.

DOI: [10.1103/PhysRevB.82.035203](https://doi.org/10.1103/PhysRevB.82.035203)

PACS number(s): 76.60.-k, 71.27.+a, 71.70.Ch

**I. INTRODUCTION**

Cerium- or uranium-based ternary compounds in the form of  $A_3T_3X_4$  (“334,”  $A=\text{Ce}$  and  $\text{U}$ ;  $T$ =transition-metal elements;  $X=\text{Sb}$  and  $\text{Bi}$ ) exhibit unusual physical properties. When  $T=\text{Ni, Pd, Pt}$ , the compounds have a trend to become so-called Kondo insulators that feature a small gap originating from the hybridization between  $f$  electrons and the conduction electrons.<sup>1</sup> One of the most extensively studied members of these compounds is the Kondo insulator  $\text{Ce}_3\text{Pt}_3\text{Bi}_4$  (Refs. 2 and 3) but there are also isostructural and isoelectric uranium counterparts,  $\text{U}_3T_3\text{Sb}_4$  ( $T=\text{Ni, Pd, Pt}$ ) (Refs. 4 and 5) and  $\text{U}_3\text{Ni}_3\text{Bi}_4$ .<sup>6,7</sup>

$\text{Ce}_3\text{Au}_3\text{Sb}_4$  also exhibits a narrow-gap semiconductorlike behavior<sup>8</sup> that looks very similar to  $\text{Ce}_3\text{Pt}_3\text{Bi}_4$  so initially it was thought to be a Kondo insulator. However, the origin of the energy gap is different than in  $\text{Ce}_3\text{Pt}_3X_4$  ( $X=\text{Sb, Bi}$ ), based on the facts that (1)  $\text{La}_3\text{Au}_3\text{Sb}_4$  is an insulator<sup>9</sup> unlike  $\text{La}_3\text{Pt}_3X_4$  ( $X=\text{Sb, Bi}$ ) that is metallic; and, (2) the Ce ion is well localized and trivalent<sup>10</sup> but mixed valence is induced in  $\text{Ce}_3\text{Au}_{3-x}\text{Pt}_x\text{Sb}_4$  and the concentration of  $\text{Ce}^{4+}$  increases with increasing  $x$ .<sup>11</sup> Therefore,  $\text{Ce}_3\text{Au}_3\text{Sb}_4$  appears to be a unique 334 compound in the sense that the  $4f$  electrons are well localized, yet similar semiconducting properties with a narrow gap<sup>12</sup> with a different origin than in Kondo insulators.

An anomalous behavior which is unsettled yet in  $\text{Ce}_3\text{Au}_3\text{Sb}_4$  is that its specific heat shows a broad peak centered at 1 K resulting in a logarithmic increase in  $C/T$ . The large electronic specific-heat coefficient  $\gamma$ , which increases up to  $\sim 4$  J/mol K<sup>2</sup> at 0.5 K, cannot be understood in a semiconductor with very low density of charge carriers. Although the transport properties are very sensitive to sample quality, the large  $\gamma$  itself at low temperature is commonly observed even in a high-quality single crystal,<sup>13</sup> indicating that the large  $\gamma$  is an intrinsic property. One scenario suggested for this observation is that a *localized* narrow  $f$  band is located at the Fermi level.<sup>13</sup> Although this can explain the large  $\gamma$  at low temperature and low carrier density simultaneously, it is not clear why the  $f$  band which is assumed to lie exactly at the Fermi level should remain localized.

Nuclear quadrupole resonance (NQR) is an ideal technique to resolve this ambiguity because it is a sensitive probe

of local spin and charge fluctuations. In this paper, we report <sup>121,123</sup>Sb NQR studies on single crystals of  $\text{Ce}_3\text{Au}_3\text{Sb}_4$ . The exact diagonalization of the crystal-electric-field (CEF) Hamiltonian gives a  $\Gamma_6$  doublet ground state, and this scheme provides excellent agreement with measurements of the uniform magnetic susceptibility, the magnetization, and the nuclear quadrupole frequency. The nuclear spin-lattice relaxation rates of both <sup>121</sup>Sb and <sup>123</sup>Sb in the temperature range 2–300 K reveal a contribution from quadrupole fluctuations at low temperatures.

**II. SAMPLE PREPARATION AND EXPERIMENTAL DETAILS**

Single crystals of  $\text{Ce}_3\text{Au}_3\text{Sb}_4$  and  $\text{La}_3\text{Au}_3\text{Sb}_4$  were grown as described in Ref. 13. In order to increase the  $rf$  penetration depth and the filling factor, the single crystals were ground into powder. Though the overall crystal symmetry of  $\text{Ce}_3\text{Au}_3\text{Sb}_4$  is body-centered cubic (space group  $I\bar{4}3d$ ), Ce and Sb atoms are located at positions that locally have tetragonal symmetry.

<sup>121</sup>Sb ( $I=5/2$ ) and <sup>123</sup>Sb ( $I=7/2$ ) NQR experiments were carried out in zero field using a conventional phase-coherent pulsed spectrometer in the range of temperature 2–300 K. The Sb NQR spectra were obtained using the Hahn echo sequence, i.e.,  $\pi/2-\tau-\pi$  with a typical  $\pi/2$  pulse length  $\sim 2$   $\mu\text{s}$  and a separation  $\tau \sim 8$   $\mu\text{s}$ . The nuclear quadrupole frequency ( $\nu_Q$ ) was determined by the separation between equally spaced transitions, as expected for axial local symmetry (anisotropy parameter  $\eta=0$ ). The nuclear spin-lattice relaxation rate ( $T_1^{-1}$ ) was measured by the saturation recovery at the  $2\nu_Q$  transition for <sup>123</sup>Sb and the  $1\nu_Q$  transition for <sup>121</sup>Sb. The relaxation data were then fitted to the appropriate equation for each transition.

**III. RESULTS AND DISCUSSION****A. Crystal-electric-field Hamiltonian**

Due to localization of the  $f$  moment of the  $\text{Ce}^{3+}$  ion in  $\text{Ce}_3\text{Au}_3\text{Sb}_4$ , one may expect that the CEF effect dominates

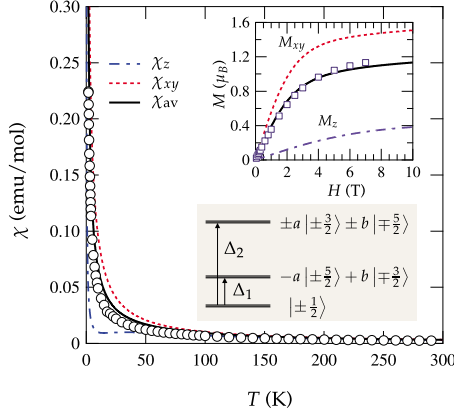


FIG. 1. (Color online) Magnetic susceptibility  $\chi$  measured at 0.1 T as a function of temperature. Magnetization  $M$  at 2 K also is shown in the inset. Dotted lines are results from CEF calculations, and their powder averages are shown as thick solid lines. The CEF level scheme is drawn with corresponding eigenstates, in which  $a = 0.7561$ ,  $b = 0.6844$ ,  $\Delta_1 \sim 25$  K, and  $\Delta_2 \sim 150$  K.

the basic magnetic and electronic properties. Indeed, two well-defined CEF transitions at 25 and 150 K were detected by inelastic neutron scattering.<sup>10</sup> The CEF Hamiltonian in tetragonal symmetry can be written as<sup>14</sup>

$$\mathcal{H}_{\text{CEF}} = B_2^0 O_2^0 + B_4^0 O_4^0 + B_4^4 O_4^4, \quad (1)$$

where  $O_l^m$  are the Stevens operators<sup>15</sup> and the CEF parameters are  $B_2^0 = 3.528$  K,  $B_4^0 = 0.244$  K, and  $B_4^4 = 2.077$  K.<sup>10</sup> By exact diagonalization of the CEF Hamiltonian, we obtained three doublet eigenstates with the ground state  $\Gamma_6 = |\pm 1/2\rangle$ . The first and second excited states were identified to be  $-a|\pm 5/2\rangle + b|\pm 3/2\rangle$  and  $\pm a|\pm 3/2\rangle \pm b|\mp 5/2\rangle$ , respectively, where  $a = 0.7561$  and  $b = 0.6844$ . The schematic CEF level diagram is shown in the inset of Fig. 1. It should be noted that the CEF  $\Gamma_6$  ground state carries the electric quadrupole moment as well as the magnetic dipole moment.

The calculated susceptibility  $\chi$  and magnetization  $M$  from Eq. (1) agree with the experimental data as shown in Fig. 1. Although the measurement was made in a single crystal, the powder averages fit the data satisfactorily because there are three local principal axes along [111] at the Ce sites.

### B. Temperature dependence of nuclear quadrupole frequency, $\nu_Q$

The NQR spectra of both  $^{121}\text{Sb}$  and  $^{123}\text{Sb}$  are shown in Fig. 2(a). A total of five lines from the two Sb isotopes is found and, as expected from the local uniaxial threefold symmetry at the Sb sites, the lines for each of the Sb nuclei are equally spaced and the nuclear quadrupole frequency,  $\nu_Q = 3e^2qQ/2h(2I-1)$ , correctly scales with the nuclear quadrupole moment  $Q$  and the nuclear spin  $I$  for the two Sb isotopes. For  $Q$ , we used the values from Ref. 16 ( $^{121}Q = -0.597 \times 10^{-28}$  m<sup>2</sup> and  $^{123}Q = -0.762 \times 10^{-28}$  m<sup>2</sup>).

We measured the temperature dependence of  $\nu_Q$  for  $^{123}\text{Sb}$ , tracking the  $2\nu_Q$  transition, which is shown in Fig. 2(b). The strong temperature dependence of  $\nu_Q$  indicates that the electric field gradient ( $eq$ ) increases with decreasing temperature.

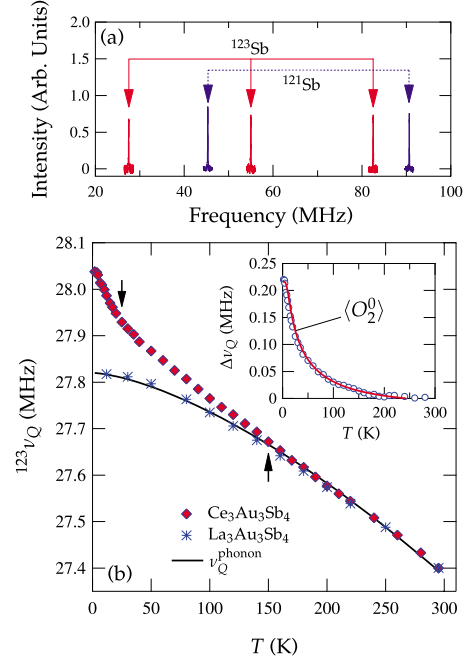


FIG. 2. (Color online) (a) Sb-NQR spectra obtained at  $T = 240$  K in zero field. Spectra of both Sb isotopes are equally spaced as expected in uniaxial symmetry. At this temperature,  $\nu_Q$  is 27.50 MHz and 45.32 MHz for  $^{121}\text{Sb}$  and  $^{123}\text{Sb}$ , respectively. (b)  $\nu_Q$  of  $^{123}\text{Sb}$  as a function of temperature. Results for  $\text{La}_3\text{Au}_3\text{Sb}_4$  which were scaled down by  $\sim 2\%$  for comparison, are shown together with the expected phonon contribution  $\nu_Q^{\text{phonon}}$ . Inset: difference between  $\text{Ce}_3\text{Au}_3\text{Sb}_4$  data and  $\nu_Q^{\text{phonon}}$ . This difference is well explained by the expectation value of the quadrupole moment  $\langle O_2^0 \rangle$  which was scaled to data.

There should be a thermal (phonon) contribution that is phenomenologically described<sup>17</sup> by the relation of  $\nu_Q^{\text{phonon}} = \nu_Q^0 - aT^{3/2}$  that is drawn as a solid line in Fig. 2(b). Clearly, there is an additional contribution below  $\sim 150$  K. For comparison, we measured  $^{123}\nu_Q$  of  $\text{La}_3\text{Au}_3\text{Sb}_4$ . Because the the temperature dependence of  $\nu_Q$  for  $\text{La}_3\text{Au}_3\text{Sb}_4$  is explained solely by the phonon contribution, the additional increase in  $\nu_Q$  for  $\text{Ce}_3\text{Au}_3\text{Sb}_4$  at low temperatures should arise from the Ce ions. We find that, as denoted by arrows in Fig. 2(b), features in  $\nu_Q$  occur at the CEF splitting energy  $\Delta_1 \sim 25$  K and  $\Delta_2 \sim 150$  K, suggesting that  $\nu_Q$  is affected by CEF splitting. This is clearly shown in the inset in which  $\Delta\nu_Q = \nu_Q(\text{Ce}) - \nu_Q(\text{La})$  is proportional to the thermal average of the expectation value of the quadrupole moment,

$$\langle O_2^0 \rangle(T) = \sum_m \frac{\langle O_2^0 \rangle_m \exp(-E_m/T)}{Z}, \quad (2)$$

where  $E_m$  and  $\langle O_2^0 \rangle_m$  are the energy and the quadrupole moment, respectively, of  $m$ th sublevel of  $J = 5/2$  and  $Z$  is the partition function.  $\langle O_2^0 \rangle(T)$  increases rapidly with decreasing temperature due to the uniaxially elongated charge distribution in the  $\Gamma_6$  ground state. A similar enhancement of  $\nu_Q$  was observed in an Sb NQR study of the skutterudite compound  $\text{PrOs}_4\text{Sb}_{12}$ , and the origin was explained by the coupling of the Sb nuclear quadrupole moment with the hexadecapole

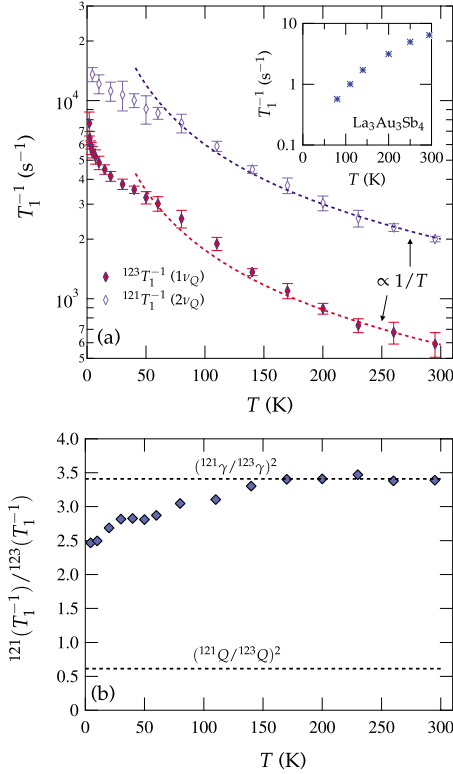


FIG. 3. (Color online) (a)  $T_1^{-1}$  as a function of temperature for both  $^{121}\text{Sb}$  and  $^{123}\text{Sb}$ . Both Sb nuclei show the same  $1/T$  dependence in the high-temperature region. At low temperatures, below  $\Delta_2 \sim 150$  K, the temperature dependence of  $^{123}T_1^{-1}$  becomes distinguished from that of  $^{121}T_1^{-1}$ . Inset:  $^{123}T_1^{-1}$  measured at  $2\nu_Q$  transition in  $\text{La}_3\text{Au}_3\text{Sb}_4$  decreases rapidly with lowering temperature. (b) Temperature-dependent ratio between  $^{121}T_1^{-1}$  and  $^{123}T_1^{-1}$ . This ratio deviates from the value expected for magnetic fluctuations, revealing a significant contribution from quadrupole fluctuations at low temperatures.

moment of  $\text{Pr}^{3+}$  ( $f^2$ ) which can have a finite thermal average, unlike other multipole moments.<sup>16</sup> Since the hexadecapole moment that requires a  $\Gamma_1$  state is not allowed in  $\text{Ce}_3\text{Au}_3\text{Sb}_4$ , the increase in  $\Delta\nu_Q$  should result from the direct coupling between the quadrupole moment of the Ce ions and the Sb nuclear quadrupole moment. We emphasize here that this direct correlation of  $\nu_Q$  with the crystal-field splittings and the quadrupole moments of an ion is extremely rare, if any, in Ce-based compounds.

### C. Nuclear spin-lattice relaxation rate and quadrupole fluctuations

So far, we have shown that the static properties  $\chi$ ,  $M$ , and  $\nu_Q$  are dominated by CEF effects. To study the local dynamics, we have measured  $T_1^{-1}$  for both  $^{121}\text{Sb}$  and  $^{123}\text{Sb}$  (Fig. 3). We find that  $T_1^{-1}$  increases rapidly with decreasing temperature for both  $^{121}\text{Sb}$  and  $^{123}\text{Sb}$ . In contrast, for  $\text{La}_3\text{Au}_3\text{Sb}_4$   $^{123}T_1^{-1}$ , which measured at  $2\nu_Q$  transition, decreases exponentially with decreasing temperature as shown in the inset of Fig. 3(a), which indicates that  $\text{La}_3\text{Au}_3\text{Sb}_4$  is a simple band-gap insulator. Therefore, the fast  $T_1$  in  $\text{Ce}_3\text{Au}_3\text{Sb}_4$  also arises from the Ce ions.

In high-temperature region,  $T_1^{-1}$  for both Sb nuclei follows a  $1/T$  dependence drawn as dotted lines in Fig. 3. The origin of this  $1/T$  dependence is not clear but it could be ascribed to hybridization between the conduction electrons and the localized  $f$  electrons in the semimetallic region at high temperatures. Alternately, if  $T_1^{-1}$  is dominated by magnetic fluctuations in a system of localized  $f$  electrons,  $T_1^{-1}$  is proportional to  $A_{\text{hf}}^2 \mu_{\text{eff}} / J_{\text{ex}}$  where  $A_{\text{hf}}$  is the hyperfine coupling constant,  $\mu_{\text{eff}}$  the effective magnetic moment, and  $J_{\text{ex}}$  the exchange coupling.<sup>18</sup> In this case, a decrease in  $J_{\text{ex}}$  with decreasing  $T$  may be responsible for the  $T$  dependence of  $T_1^{-1}$ .

In the temperature region below  $\sim 150$  K, the temperature dependence of  $T_1^{-1}$  for the two Sb isotopes become different, which is more prominent below  $\sim 25$  K. In general,  $T_1^{-1}$  due to spin fluctuations is written as<sup>19</sup>

$$T_1^{-1} \propto T \gamma_n^2 \sum_q A_{\text{hf}}^2(q) \chi''(q, \omega_0), \quad (3)$$

where  $\gamma_n$  is the nuclear gyromagnetic ratio,  $A_{\text{hf}}(q)$  the  $q$ -dependent hyperfine coupling constant, and  $\chi''$  the imaginary part of the dynamic susceptibility. Since the ratio of  $T_1^{-1}$  for the two Sb isotopes is the same as  $(^{121}\gamma_n / ^{123}\gamma_n)^2 = 3.41$ , as shown in Fig. 3(b), we conclude that magnetic fluctuations from Ce ions are the major contribution to relaxation processes at high temperatures, regardless of the origin of  $1/T$  behavior.

The ratio  $T_1^{-1}$  for the two isotopes deviates from 3.41 below  $\Delta_2 = 150$  K toward the value expected for the ratio of the square of quadrupole moments  $(^{121}Q / ^{123}Q)^2$ . This observation appears to be consistent with the enhancement of  $\nu_Q$  at low temperatures. This trend is even more prominent below  $\Delta_1$ . In this temperature region,  $^{123}T_1^{-1}$  shows an almost diverging behavior while  $^{121}T_1^{-1}$  increases more weakly down to 4 K. Unfortunately,  $T_1$  is too short to measure below 4 K and 2 K, for  $^{121}\text{Sb}$  and  $^{123}\text{Sb}$ , respectively. Further, due to the shortening of  $T_2$ , the signal becomes very weak. Nevertheless, the different temperature dependences of the two isotopes indicate the important role of quadrupole fluctuations in the spin dynamics at low temperatures. However, this apparent contribution of the quadrupole fluctuations to the nuclear relaxation is incompatible with the fact that  $\Gamma_6 = |\pm 1/2\rangle$  state alone cannot produce the quadrupole fluctuations due to the Kramers degeneracy of the ground state.<sup>20</sup> Here, we conjecture a finite matrix element between  $\Gamma_6$  and the first excited doublet forming an effective ‘‘quartet’’ state. In this case, broadening of the levels, for example, due to anharmonic phonons<sup>21</sup> may help promote the mixture of the two doublet states. We recall a similar situation in a Yb-monopnictide YbSb whose ground state is also a  $\Gamma_6$  doublet that consist of  $|\pm 1/2\rangle$  and  $|\mp 7/2\rangle$ . YbSb shows a phase transition at 5 K and quadrupole order has been suggested as its origin, even with a Kramers ground doublet, which has no quadrupole moment, separated by rather large splitting energy of 170 K with the first excited states.<sup>22,23</sup> In our case, in comparison with YbSb, a mixed quadrupolar interaction seems to be more realistic since the  $\Gamma_6$  in  $\text{Ce}_3\text{Au}_3\text{Sb}_4$  has a quadrupole moment and the splitting energy to the first excited states is much smaller than that of YbSb.

The almost diverging  $T_1^{-1}$  of  $^{123}\text{Sb}$  resembles critical slowing down near an ordering temperature and, indeed, specific-heat measurements find a clear anomaly at 0.2 K. From magnetic field dependence of the specific heat, the anomaly appears to be antiferromagnetic in nature.<sup>24</sup> Although AFM order appears to be primary, the additional quadrupole contribution may be detected by the specific heat, and the coupled magnetic and quadrupolar interactions may lead to the observed large  $C/T$  at low temperatures. In order to pin down the nature of the transition at 0.2 K, magnetization measurements at low temperatures are needed. Regardless of the detailed nature of the transition, the temperature dependence of both  $T_1^{-1}$  and  $\nu_Q$  imply a strong coupling between the quadrupole moment of the Sb and the quadrupole moment of Ce in the CEF scheme.

#### IV. CONCLUSION

In conclusion, we have measured Sb NQR in the narrow-gap semiconductor  $\text{Ce}_3\text{Au}_3\text{Sb}_4$  and have shown that the static ( $\nu_Q$ ) and dynamic ( $T_1^{-1}$ ) properties of  $\text{Ce}_3\text{Au}_3\text{Sb}_4$  are affected strongly by the crystal-electric-field splitting. The nuclear quadrupole frequency  $\nu_Q$ , after subtracting the phonon contribution, increases with decreasing temperature in proportion to the expectation value of the quadrupole moment of the Ce

ion. This reveals a clear coupling between the quadrupole moment of Ce and the nuclear quadrupole moment at Sb. Furthermore, quadrupole fluctuations contribute to  $T_1^{-1}$  at low temperatures in addition to magnetic fluctuations that are dominant. This finding strongly suggests the finite matrix element between the  $\Gamma_6$  ground doublet and the excited doublet through intersite quadrupole-quadrupole interactions since the Kramers degeneracy does not allow the quadrupole fluctuations. From our NQR results, we propose that the anomalous divergence of  $C/T$  at low temperatures may arise from the quadrupole fluctuations.

We have shown that  $\text{Ce}_3\text{Au}_3\text{Sb}_4$  is a special member of the 334 family, not only due to its well localized  $f$  moment with narrow-gap, semiconductorlike behavior but also to the strong influences of crystal electric fields on the static and the dynamic local properties. It deserves further detailed experimental and theoretical studies to elucidate the role of quadrupole moments and their fluctuations in determining physical properties.

#### ACKNOWLEDGMENTS

We thank V. Kataev, S. Kambe, and Y. Tokunaga for the useful suggestions and discussions. Work at Los Alamos National Laboratory was performed under the auspices of the U.S. Department of Energy, Office of Science.

\*Present address: IFW-Dresden, Institute for Solid State Research, Dresden, Germany; sbaek.fu@gmail.com

<sup>1</sup>G. Aeppli and Z. Fisk, *Comments Condens. Matter Phys.* **16**, 155 (1992).

<sup>2</sup>M. F. Hundley, P. C. Canfield, J. D. Thompson, Z. Fisk, and J. M. Lawrence, *Phys. Rev. B* **42**, 6842 (1990).

<sup>3</sup>A. P. Reyes, R. H. Heffner, P. C. Canfield, J. D. Thompson, and Z. Fisk, *Phys. Rev. B* **49**, 16321 (1994).

<sup>4</sup>T. Takabatake, S. Miyata, H. Fujii, Y. Aoki, T. Suzuki, T. Fujita, J. Sakurai, and T. Hiraoka, *J. Phys. Soc. Jpn.* **59**, 4412 (1990).

<sup>5</sup>T. Endstra, G. J. Nieuwenhuys, J. A. Mydosh, and K. H. J. Buschow, *J. Magn. Magn. Mater.* **89**, L273 (1990).

<sup>6</sup>T. Klimczuk *et al.*, *Phys. Rev. B* **77**, 245111 (2008).

<sup>7</sup>S.-H. Baek, N. J. Curro, T. Klimczuk, H. Sakai, E. D. Bauer, F. Ronning, and J. D. Thompson, *Phys. Rev. B* **79**, 195120 (2009).

<sup>8</sup>M. Kasaya, K. Katoh, and K. Takegahara, *Solid State Commun.* **78**, 797 (1991).

<sup>9</sup>K. Takegahara and Y. Kaneta, *Prog. Theor. Phys.* **108**, 55 (1992).

<sup>10</sup>D. T. Adroja, B. D. Rainford, Z. Hossain, E. A. Goremychkin, R. Nagarajan, L. C. Gupta, and C. Godart, *Physica B* **206-207**, 216 (1995).

<sup>11</sup>K. Katoh and M. Kasaya, *J. Phys. Soc. Jpn.* **65**, 3654 (1996).

<sup>12</sup>S. Kimura, Y. Sato, F. Arai, K. Katoh, M. Kasaya, and M. Ikezawa, *J. Phys. Soc. Jpn.* **62**, 4174 (1993).

<sup>13</sup>H.-O. Lee, Y.-J. Jo, L. Balicas, P. Schlottmann, C. L. Condon, V. A. Sidorov, P. Klavins, S. M. Kauzlarich, J. D. Thompson, and Z. Fisk, *Phys. Rev. B* **76**, 155204 (2007).

<sup>14</sup>M. T. Hutchings, in *Solid State Phys.*, edited by F. Seitz and D. Turnbull (Academic, New York, 1965), Vol. 16, p. 227.

<sup>15</sup>K. W. H. Stevens, *Proc. Phys. Soc., London, Sect. A* **65**, 209 (1952).

<sup>16</sup>H. Tou, M. Doi, M. Sera, M. Yogi, H. Sugawara, R. Shiina, and H. Sato, *J. Phys. Soc. Jpn.* **74**, 2695 (2005).

<sup>17</sup>E. N. Kaufmann and R. J. Vianden, *Rev. Mod. Phys.* **51**, 161 (1979).

<sup>18</sup>T. Moriya, *Prog. Theor. Phys.* **16**, 641 (1956).

<sup>19</sup>T. Moriya, *J. Phys. Soc. Jpn.* **18**, 516 (1963).

<sup>20</sup>A. Abragam and B. Bleaney, *Electron Paramagnetic Resonance of Transition Ions* (Clarendon, London, 1970).

<sup>21</sup>P. Thalmeier, *J. Phys. C* **17**, 4153 (1984).

<sup>22</sup>K. Hashi, H. Kitazawa, A. Oyamada, and H. A. Katori, *J. Phys. Soc. Jpn.* **70**, 259 (2001).

<sup>23</sup>A. Oyamada, S. Maegawa, T. Goto, K. Hashi, and H. Kitazawa, *J. Phys. Soc. Jpn.* **73**, 1953 (2004).

<sup>24</sup>N. Kurita (unpublished).